12-2021

How Salivary Glands Recover from Fibrotic Injury

Gabriella Majka

How Salivary Glands Recover from Fibrotic Injury

An honors thesis presented to the
Department of Biology,
University at Albany, State University of New York
in partial fulfillment of the requirements
for graduation with Honors in Biology
and
graduation from The Honors College

Gabriella M Majka

Research Mentor: Amber Altrieth, M.S.

Research Advisor: Melinda Larsen, Ph.D.

December 2021

Abstract

Extracellular matrix deposition is required for repair after injury, but if left unresolved can result in fibrosis. Fibrosis is an excess deposition of extracellular matrix proteins following injury or aging that leads to eventual organ dysfunction. One surgical model that we have used to study mechanisms of fibrosis is the salivary gland ductal ligation model. During the process of ligation, a clip is placed on the main ducts of the submandibular (SMG) and sublingual gland (SLG) which leads from the salivary glands to the mouth. This causes the gland to atrophy, or waste away, resulting in decreased acinar cell differentiation and death. In the salivary gland, the acinar cells are cells that line an acinus, which is a small sac-like cavity in the gland into which saliva is secreted. We can detect loss of acinar cells by immunostaining to detect epithelial cell proteins like aquaporin 5 (AQP5) which is a water channel protein or conavalin A (ConA). EpCam-FITC can be used to stain for epithelial cells and Ki67 is a cell proliferation marker that allows us to observe what cells are proliferating. The longer the clip is held in place during ligation, the more fibrotic the stroma becomes and the smaller and less productive the salivary gland will become. The ductal ligation can also serve as a model for recovery from injury following the removal of the clip, or deligation. Based on previous research in which saliva production was measured following deligation, acinar cells can fully recover. AQP5 has also been observed in deligated samples, suggesting that the acinar cells do regenerate during deligation. It is unknown how quickly after injury the gland begins to recover, and if the dissipation of the fibrotic response precedes restoration of function. We hypothesize that following deligation, ECM levels will decrease, prior to the restoration of acinar marker protein expression. To address this, we will be performing immunofluorescent and histological staining, IHC, on ligated and deligated tissue cryosections. In this study we will be using C57 mice with a deligation point or mock surgery point of 3 days. First, we will determine if and when acinar cell markers, such as AQP5 and ConA return following deligation. Second, we will be examining the endothelia cells following deligation via IHC staining with CD31 and EpCam-FITC. Lastly, we will be observing what cell types are proliferating with the marker Ki67. This study will provide information on the timing of salivary gland recovery from traumatic injury, which may provide insights into possible regenerative therapies. Depending on the results of this study, we can modify our ligation/deligation timeline to be potentially shorter than 3 days, or longer than 7 days.

Keywords: *Proliferation, Fibrosis, Immunohistochemistry, Trichrome, Fibrosis*

Acknowledgments

I would like to thank the members of the Larsen Lab, especially Amber Altreith and Dr. Larsen for giving me the opportunity to be emersed in the world of cellular biology research and encouraging me to produce the best work that I can. I would also like to thank my family and friends for always supporting me throughout my undergraduate education and pushing me to reach my goals. I could not have done any of this without all of this constant support and admiration and I am grateful for everyone who has been with me on my journey thus far.

List of Figures

List of Tables

Table of Contents

Chapter 1: Introduction

There are three pairs of major salivary glands in mammals: the submandibular (SMG), the sublingual (SLG), and the parotid. All three types of glands are similar in structure, in that the branched ductal system opens up into the oral cavity with saliva being produced by the acini, which are the secretory endpieces (Holmberg & Hoffman, 2014). These acinar cells are in the epithelial compartment of the salivary glands. The epithelial compartment also includes ductal cells and myoepithelial cells. The ductal cells transport and modify the saliva, and the myoepithelial cells aid in the secretion of saliva from the acinus. The epithelial compartment is surrounded by the stromal compartment. The stromal compartment includes neurons, extracellular matrix, endothelial cells, and immune cells. In a healthy mammal, these cells aid in the creation and production of saliva.

Saliva is important for speech, chewing, and digesting food. The presence of saliva also protects the mouth from oral infections and cavities. Without the production of saliva, eating dry foods can become dangerous, because our mouths would be more prone to infection and, if severe, loss of saliva can even cause loss of taste. Salivary gland hypofunction causes a decrease in normal gland function, decreasing saliva flow. Hyposalivation can be caused by disease treatments like irradiation therapy for head and neck cancer and chemical factors like certain medications. Hyposalivation can also induce gastrointestinal (GI) complications such as pain, due to the dryness of the pharynx and esophagus, and nausea (Tincani et al., 2013).

One disease that can cause hyposalivation is Sjogren's syndrome (SS). SS is an autoimmune inflammatory disorder that mainly impacts the salivary glands and other related glands. SS presents itself as the combination of both xerophthalmia (dry eyes) and xerostomia (dry mouth). Xeropthalmia can give rise to many optical issues, such as ulcers and infections and

xerostomia can give rise to difficulty swallowing, and dental issues. This type of autoimmune disorder typically requires a predisposed genetic background, but the exact etiology is unknown. Certain autoantibodies are present in the majority of SS cases, and they are rheumatoid factor (RF), anti-nuclear antibodies (ANA), but there has not been enough research to conclude if these can be markers for the development of SS. This disease can present by itself, which is called primary Sjogren's syndrome (pSS), or it can present alongside other connective tissue diseases like rheumatoid arthritis (RA) or lupus, which is known as secondary SS. In the category of autoimmune rhematic diseases, SS is the second most common disease, and it mostly impacts women. Past studies have indicated that certain infections may have a protective role against the development of SS, but the particular way in which infections play a role in the development of SS is unknown. One main finding is that patients with low vitamin D levels have more adverse reactions when diagnosed with SS. This outcome can aid researchers in determining if vitamin D levels play a role in disease development and how they can be used in disease treatment. In addition to the various symptoms seen in SS patients, another very frequent symptom can be fatigue. The type of fatigue that is seen in SS patients is physical and somatic rather than a mental fatigue (Tincani et al., 2013). This disorder is mainly managed by rheumatologists; however, they work in conjunction with other specialists like ophthalmologists and oral medicine specialists.

In addition to the more common symptoms above, physicians also have to pay attention to their patients' vasculature. In the vascular system, the microvasculature is typically affected in autoimmune and connective tissue disorders. One way to non-invasively assess the microvasculature is through nailfold capillaroscopy. One main characteristic that is found in several autoimmune disorders is a scleroderma pattern (Tektonidou et al., 1999). Scleroderma is

caused by an over production of collagen in the skin, and it causes a tightening and hardening of the skin and other connective tissues. One way that scleroderma can reveal itself is through Raynaud's phenomena (RP), and in approximately 30% of SS patients have this phenomenon. Capillaries were examined in multiple SS patients; some had RP and others did not. In the SS patients that did not have RP, their capillary density was not significantly changed, and in SS with RP, their capillary density was significantly lower than the control group (Tektonidou et al., 1999). Demirci et al. (2016), conducted a study in which they examined the vasculature of female patients with primary SS. One way to observe atrial stiffness is via the blood pressure, a patient with stiff arteries will have a higher-than-normal systolic blood pressure and a lower diastolic. Since SS shares many of the same serologic features with rheumatoid arthritis and lupus, which are both illnesses that include the presence of stiffened arteries. Demirci et al. (2016), conducted this study because in previous studies it has been noted that in SS there is increased endothelial dysfunction and atherosclerosis, or narrowing of the arteries; however, there was not any mention of arterial stiffness. They were able to conclude that in a subset of SS patients, there is increased arterial stiffness compared to control populations. Atherosclerosis has also been suggested to be mediated from immune processes due to patients with autoimmune diseases having increased rate of narrowing vessels. In patients with SS, chronic inflammation can be one of the main reasons for the increased amounts of atrial stiffness. Both of these studies strongly suggest that in a subset of SS patients who have reduced micro vessel density, abnormal vessels, and increased amount of atherosclerosis, endothelial cell dysfunction could be contributing to salivary gland hyposalivation.

Although there are several common characteristics which can be used to diagnose SS patients, until 2016 there was not a validated set of criteria across the globe for individuals with

SS. In 2016, a paper was released with the intent to create a validated set of classification criteria for diagnosing SS that would be recognized by the American College of Rheumatology (ACR) and also by the European League against Rheumatism (EULAR). Prior to this study different organizations had different methods for testing their suspected SS patients the ACR would only focus on objective tests whereas other organizations would use other symptoms like dry eyes. This study concluded that in addition to the past requirements to obtain a SS diagnosis, oral and/or ocular symptoms, patients must also have one of the following symptoms: having anti-SSA autoantibodies, an ocular staining score greater than or equal to 5, a Schirmer score of greater than or equal to 5, and an unstimulated whole saliva flow rate (UWS) of less than or equal to 1. These 5 different criteria are all summed and weighted together, and if the patient has a total score of greater than or equal to 4, they meet the criteria to be diagnosed with SS (Shiboski et al., 2016). In order to ensure the correct weighting of these various components to SS, there has to be specific ways in which to measure each symptom. For dry eyes, it is categorized as a complex syndrome that impacts the tear film. Damage to this impacts the amount of tear production, which causes extreme discomfort and even damage to the eye. The type of dry eye as seen in SS patients is categorized as aqueous-deficient dry eye, due to lack of tear production (Tincani et al., 2013). The traditional way to diagnosis SS has been via biopsy of the salivary glands. Even though these give accurate results, this is an invasive and potentially dangerous procedure (Niemla et al., 2004). However, only a select few physicians will harvest the salivary gland and therefore collect the saliva of a potentially ill patient. The saliva can tell a researcher a lot about what medical condition a person has, or what their physiological state is, so testing the quality and quantity of saliva is important is detecting diseases like SS (Iorgulescu, 2009).

In addition to all of the biological and molecular factor that can influence the appearance of SS, hyposalivation does have other causes. Hyposalivation can also be caused by certain medications. In a 2017 study conducted by Tan et al., the risk of hyposalivation, as a side effect of certain drugs, was researched. This study reviewed articles from 1990 up until 2016 that included any data on dry mouth, salivary gland function, medication use, and the elderly population. Typically, older adults, aged 60 years or older, tend to take more medications than the average adult. 40% of the elderly that live in normal communities and approximately 75% of those who are living in a facility take five or more medications. The mixture of all of these treatments and the presence of co-morbidities in older adults can increase their risk of adverse side effects to medications. The most common of these adverse effects is hyposalivation. Xerostomia is the subjective feeling of dry mouth, but it does not necessarily mean that the glands are not producing enough saliva. In past studies it has been proven that increased medication usage leads to and causes hyposalivation, but the severity has not been studied. The exact mechanisms in which medications can lead to hyposalivation varies, but the main causes are dehydration, an imbalance in electrolytes, and vasoconstriction in the glands themselves. The main classes of drugs that can induce dry mouth in individuals are antidepressants, antipsychotics, antihistamines, sedatives, medicines to regulate high blood pressure (antihypertensives), medications that inhibit the actin of acetylcholine (anticholinergics), and cancer therapeutics.

Another type of disease that is known to induce hyposalivation is cancer, specifically head and neck cancers. Head and neck cancers can involve the salivary glands, and treatment for head and neck cancers can itself cause salivary hypofunction. Head and neck cancer is categorized by a board range of tumors that can form anywhere from the upper digestive tract,

sinuses, salivary glands, or thyroid glands. In the past two decades the number of smokers has been on a decline, and in direct correlation from this, the cancer incidence rates have also declined. Also, in the past two decades racial disparities in cancer treatment and outcomes have begun to decline. (Siegel et al., 2017). In 2017, there were 49,670 new cases of oral cavity and pharynx cancers across both sexes. Men have a higher incidence and mortality rate of oral cavity and pharynx cancers than women. For patients that have head and neck cancer, their treatment plan is often multidisciplinary. Traditionally, surgery is done first and then followed by radiotherapy. Unfortunately, the radiation treatment lowers a patient's quality of life due to its complications. Depending on the specific location of the tumor, the corresponding treatment changes, this is because certain locations are inoperable, so radiation is the only option. Some of the main complications of radiation can be inflammation of the mucosal membranes, which can cause sore throat and mouth. Some other implication can be the damage to the "sweet tasting" taste buds, skin irritation, hair loss and loss of sweat and sebaceous gland function. However, one of the main causes to a lesser quality of life can be the extracting of teeth prior to radiation therapy. Teeth are extracted if they are deemed non-viable for the long term. Another complication is edema of the larynx which can cause hoarseness and airway obstruction. All of these complications happen fairly early on in treatment; however, there are many long-term effects as well. Xerostomia, dental caries, bone necrosis and several other serious side effects can stay with these patients for years after treatment (Yeh, 2010). During radiation treatment for head and neck cancer, there tends to be an increase in fibrotic tissue in the salivary glands. Fibrosis in the salivary glands can cause the issue of hyposalivation in patients. The fibrotic tissue impacts the gland function, thus increasing the adverse side effects from the radiation therapy.

Current treatments for hyposalivation are only palliative, so the discovery of new regenerative therapies is needed. According to Wu in 2015, there are different classes of treatments, the first one aims to increase saliva flow using medication. Muscarinic agonists such as, pilocarpine, cevimeline, and bethanechol, can be prescribed to stimulate an increase in salvia production. However, the salvia produced via this route does not contain the proteins that naturally produced salvia contains. So, although these agonists can increase salvia flow, it is unknown if they aid in halting the dental issues. This type of treatment is typically given in pill form and can noticeably begin working in less than an hour. However, after three to four hours, the pills' effects wear off, and another needs to be taken. These muscarinic agonists, typically have some adverse side effects such as sweating, decreased depth perception, diarrhea, and increased urination. In addition to these side effects, this treatment can become costly, depending on the specific drug used. There are, however, non-pharmacologic methods to increasing salvia production. Sugar free gum and hard candies can be used because they are masticatory/gustatory stimuli. This means that they appear to aid in the stimulation of saliva, however, they only add in the production of saliva while the object is in the patient's mouth. Meaning that once you finish a piece of sugar free gum, you would need to begin chewing another piece, or your saliva flow will decrease. The third way to increase saliva flow is to use wetting agents, such as salvia substitutes. One type of wetting agent is the line of Biotene products, which can come in gel or spray form. Water is most commonly used; some patients will even add oil to their water. In the case of both wetting agents, they are not long lasting, and there is still not enough information to state how effective the treatment is (Wu, 2015). In addition to approved treatments, newer experimental treatments involving stem cells are being tested. Xu et al. (2012), released an article testing mesenchymal stem cells (MSCs) in those with SS and how MSCs can be used as

treatment. MSCs are multipotent stem cells, with the ability to differentiate into a variety of cells. In patients with SS, the MSCs in the bone marrow were defective and unable function normally. It was determined via experiments on mice and human trials, that MSC treatment can suppress the autoimmunity seen in SS and restore salivary gland function. Although this is not FDA approved, this treatment has also been shown to be effective in the treatment of type 1 diabetes and lupus.

To further examine hyposalivation and SS, the salivary glands have to be examined on a cellular level. Endothelial cells (ECs) are cells that are found lining the blood vessels and as seen in previous studies, have been deemed a requirement for the epithelial patterning of the salivary gland created during the process of vasculogenesis (Kwon et al., 2017). Forming new blood vessels via angiogenesis is critical for the upkeep and regulation of the organ systems in the body. ECs are also important in the growth of many tissues through the secretion of paracrine acting factors, including growth factors, cytokines, chemokines, and ECM components called angiocrine factors. Past research has determined that these angiocrine factors are derived from activated ECs. Activated ECs are important in relaying the injury-induced angiocrine factors to the tissue specific stem cells to push along the process of regeneration. Past regeneration studies have focused on the liver. The regeneration of the liver has well defined set points and is able to fully restore the liver back to its original mass prior to resection surgery. In order to determine how the angiocrine factors relate to regeneration, a surgical resection of 70% of the liver's mass was performed. One to four days after this resection, is known as the initial angiogenesis-independent inductive phase. During this phase the non-proliferating liver ECs begin to stimulate hepatocyte growth factor (HGF). The next time frame is four to twelve days following surgery. During this phase, the liver ECs stimulate the blood vessels to begin proliferating. During this

study it was also determined that ECs, derived from the bone marrow that co-express CD31 and are able to produce HGF, can be placed into the liver to aid in a faster regeneration. In regard to phase two of liver regeneration, this is when the blood vessels begin to proliferate, and growth factors begin to rise to their basal levels. Liver ECs are also able to stimulate recovery through the process of fibrosis. When the bile-duct is ligated, certain receptors can be either repressed or upregulated with leads to the fibrosis of the liver tissue. This data confirms that liver ECs control regeneration and homeostasis because they are able to guide other cells and receptors in the organ when injury or disruption in homeostasis occurs. In addition to the liver, pancreatic studies have been done with the purpose of trying to resolve the disease of diabetes, lung studies observing restoration of lung epithelium and cardiac repair have been studied (Rafii et al., 2016). In addition to maintaining homeostasis, angiocrine factors have been shown to aid the organ repair from injury. ECs are able to induce organogenesis before angiogenesis and with collaboration of trophogens, or a substance that impacts the growth of an organ. This study once again used a 70% resection surgery of the liver in order to observe regeneration. Once the surgery is performed, the ECs are able to stimulate growth factors with through the release of trophogens. This allows for the liver to begin regenerating. Angiocrine factors have been shown to be tissue specific (Ding et al., 2010) and to change in response to different types of injury (Rafii, 2016). No previous studies have looked into angiocrine factor production in the salivary gland or the impact of ECs on salivary gland regeneration.

To study mechanisms through which glands can recover from injury, the salivary gland ductal ligation model has been developed (Woods et al., 2015). During the process of ligation, a clip is placed on the main ducts of the submandibular (SMG) and sublingual gland (SLG) which leads from the salivary glands to the mouth. The main excretory duct of the SMG is the

Wharton's duct and the main excretory duct of the SLG is the Bartholin's duct. These two excretory ducts meet and connect at the sublingual caruncula (Holmber & Hoffman, 2014). In Cotroneo et al., 2008 they describe the ligation model. First the mice are dosed with anesthesia (ketamine and xylazine) and through a small incision in the bottom of the mouth the excretory ducts were clipped with a metal clip. The incision was then sutured. Then two weeks later the mice were placed under anesthesia again and the clip was removed. Depending on the condition the glands were removed immediately or after another few days. This surgery protocol was previously done in other studies and has been shown to cause injury to the glands. During ligation, extracellular matrix deposition (ECM) increases, causing a reversible fibrosis injury that affects gland function. Fibrosis is an excess deposition of extracellular matrix that occurs following injury, which can be detected by Masson's trichrome stain. With fibrosis, the acinar cells begin to atrophy as acinar cell loss occurs. The longer the clip is held in the place during ligation, the smaller and less productive the salivary gland will become. Previous research conducted by Cotroneo et al in 2008 observed that following ligation, the salivary glands weighed 50% less than the control glands (unoperated) and for the glands that were deligated 3 days following ligation, the glands began to increase in weight. It was also observed that in the ligated glands, hematoxylin, and eosin (H & E) staining suggests that the majority of the acini have disappeared and, through alcian blue/ periodic acid schiff (AB/PAS) staining, the majority of secretory granules were also gone. After three days, through H&E staining, the acini began to recover in the SMG and SLG glands, mainly around the edges of the gland. Through the AB/PAS staining, the glycoprotein content in the acini cells began to return as well; the water channel protein, aquaporin 5 (AQP5), expression began to increase again in areas where there were acini. Ki67, a cellular proliferation marker, was not present in the ligated glands, but once

deligated Ki67 positive nuclei were present suggesting that cells are beginning to proliferate again. Most previous studies are done in mice, however in 2021 Lutitje et al., examined human SMG glands, after radiation therapy (RT). They discovered that following that RT treatment, the SMG had a near complete loss of acinar cells in that acinar cell that expressed functional secretory markers did remain present in the glands. The ligation model mimics a similar fibrotic response as to what occurs following radiation surgery phenotypes seen in humans are also seen in mice with this model.

Deligation is the removal of the clip placed on the duct. Based off previous research, following deligation, acinar cells can fully recover (Cotroneo, 2008). This data is based off saliva samples, as saliva production is an indicator of functional acinar cells. During deligation, the level of functional acini in the salivary gland will begin to increase and the amount of cell inflammation and fibrosis decreases. Previous work demonstrated that the amount of trichrome staining decreases after deligation.

The main overall goal of our research is to determine how fibrosis contributes to or hinders salivary glands regeneration following trauma, since this information can be useful in developing therapeutics for treatments of diseases like SS where salivary hypofunction occurs. We want to examine two main questions in my research; the first is what is the timing of the decrease in ECM and the increase in acinar cells following deligation? Second, we ask what is the timing of endothelial cell proliferation following deligation? As endothelial cells contribute to regenerative responses through production of angiocrine factors, which occurs prior to their proliferation, understanding when their proliferation occurs during gland recovery is critical, I hypothesize that once the vasculature clip is removed, the increased presence of pro-regenerative angiocrine factors will aid in the regeneration of salivary glands. In our study, we will be able to

identify when endothelial cells are recovering and when acinar cells are recovering following removal of the clip. I will use immunofluorescence staining on mice that have been ligated compared to mice that have gone through deligation to observe how the levels of each cell type change using CD31 as an endothelial maker, and EpCam-FITC as an epithelial cell marker. Ding et al. (2010), found that at in the first three days following injury, liver cells are actively dividing to replace cells following a liver resection. After this initial division of cells, the endothelial cells begin to divide in order to provide nutrients to the growing tissue. We want to examine these timepoints, 3 day and 7 days post injury and observe if this trend also occurs in salivary glands. This will allow us to determine when the switch between salivary gland cells proliferation and endothelial cells proliferation occurs.

The work in this paper was performed in collaboration with the following graduate students in Dr. Melinda Larsen's laboratory: Amber Altrieth and Kevin O'Keefe. Kevin O'keefe performed ductal ligation surgeries and processed tissue samples. Amber Altrieth performed surgeries, processed the resulting tissue samples, and saliva collection. She also supervised the immunostaining and image quantification that I performed. I assisted Amber with the surgeries and saliva collections.

Chapter 2: Materials and Methods

2.1 Mouse Strains and Husbandry

All animal husbandry and procedures were performed in accordance with protocols approved by the University at Albany, SUNY IACUC committee and housed in 12-hour light/dark cycle with access to water and dry food. C57BL/6J mice were ordered from the Jackson Laboratory (Jackson Laboratory #000664) and were given a unique identifier prior to surgery.

2.2 Ductal Ligation and Deligation Surgery

For the experiments in chapter 3, 12-week-old C57BL/6J female mice were weighed, ear-punched and given ketamine/xylazine, an anesthetic, to sedate them before the surgery. Anesthesia consisted of injecting the mice intraperitoneally (IP) with a solution of 100mg/kg of Ketamine and 20mg/kg of Xylazine at a dose of 0.1mL/10g of body weight stock solution. Once the mice were sedated, they were injected subcutaneously with a pain medication composed of 100 µL of 0.015 mg/mL buprenorphine stock solution and secured on the surgery station. Nair was used to remove the hair from the mouse's neck, and a combination of betadine and ethanol was used repeated three times to sterilize the skin for surgery. A surgical drape was then placed over the mouse, and after a toe pinch to ensure the sedation of the mouse, surgery began. Scissors were used to make an incision on the neck of the mice, just offset from the midline, and a combination of forceps and scissors were used to find the salivary glands. Once the glands were located, the clear duct of the SMG and SLG was clipped with a vasculature clip. Once the ducts were clipped, the mouse was sutured and placed in a clean cage on top of a warming pad until recovery from anesthesia. This clip remained on for 14 days. After 14 days mice were either

harvested or were sedated again, and the vasculature clip was removed for 3 days, or 7 days prior to harvest. For the mock surgery mice, the ducts were located but no clip was put into place.

Figure 1

Ductal Ligation Surgery Model

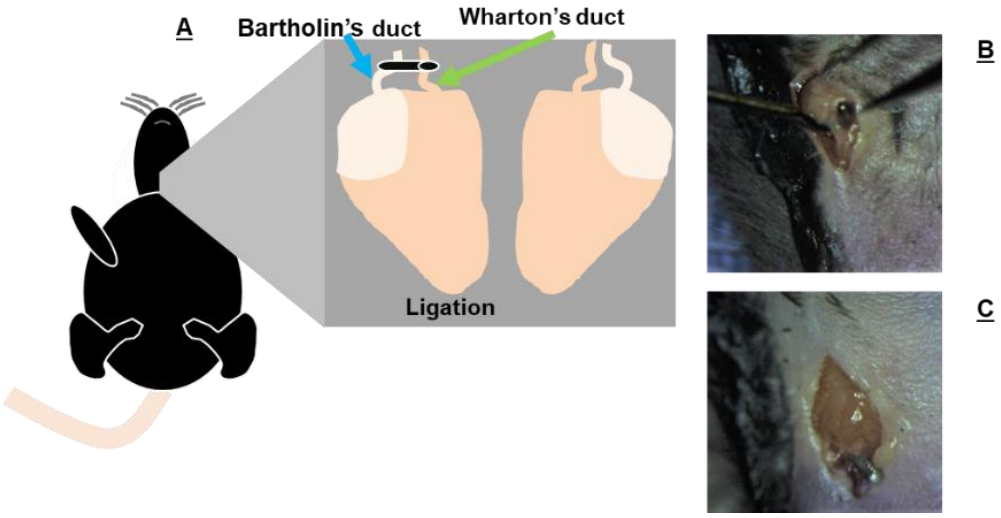

Note: **Figure 1A**, is a cartoon depicting the mouse salivary gland ductal ligation injury model. It allows us to induce a reversible fibrosis injury to study the mechanisms through which salivary glands can reverse fibrosis. During ligation in surgeries that were performed by Amber Altrieth, a metal clip is placed on the ducts of the left submandibular (SMG) and sublingual gland (SLG) which causes the gland to fibrosis (shown by increased ECM) and gland atrophy with loss of differentiation of the acinar cells that make saliva. In a negative control mock surgery, an incision is made, and Amber will locate the salivary gland and the corresponding ducts; however, there is no clip placed**. Figure 1B**, is an image taken from a ductal ligation surgery, in which the duct is hooked around the instrument. **Figure 1C**, is an image of the metal clip placed on the ducts.

2.3 Saliva Collection

A rolled-up cotton pad was placed inside a 0.6mL centrifuge tube with a hole in the bottom that is inside a 1.75mL centrifuge tube. These tubes were all pre-weighed and labeled prior to the experiment. Selected mice were weighed and administered 100mg/kg of Ketamine and 20mg/kg of Xylazine at a dose of 0.1mL/10g of body weight stock solution. After a wait

time of 3 minutes, we administered a paw pinch to ensure the mice were sedated. The mice were then restrained on a clean surface using a 50mL conical tube with a hole cut at the bottom. A heating pad was placed on the surface and the tube was tilted 60 degrees. Pilocarpine (0.375mg/kg from a 3.75mg/mL stock solution) was given via an IP injection. After waiting 3 minutes, or when the saliva began to flow, whichever came first, a rolled-up cotton pad was placed in the mouth of each mouse. The saliva was collected into this pad. The cotton pad stayed in the mouth of each mouse for 15 minutes. The cotton pad was then removed and placed into the pre-weighed tubes. The tubes were then re-weighed to quantify the total weight of saliva collected. Centrifuging the tubes allowed for the saliva to be collected into the 1.75 mL microcentrifuge tube and measured via a pipette. 0.25mL of sterile saline was then administered subcutaneously (SC) to prevent dehydration and the mice were kept warm until they were able to ambulate. Once the mice were fully awake, they were placed back in their cages.

2.4 Tissue processing and Cryosectioning

Once glands were removed from the mice, they were placed in 4% paraformaldehyde (PFA) diluted in 1xPhosphate buffered saline (PBS) for two hours at a temperature of 4 degrees Celsius. The glands were then washed three times in a 1x PBS solution before being placed into various sucrose solutions, 5%, 10%, and 15% each for one hour at 4 degrees Celsius. After these three steps, the glands were placed in a 30% sucrose overnight at 4 degrees Celsius. The next day, an equal volume of optimal cutting temperature (OCT) tissue freezing medium was added to the glands, creating a 50% OCT 15% sucrose solution, where the glands were kept overnight at 4 degrees Celsius. The next day, the glands were frozen indirectly over liquid nitrogen. After five minutes, the samples were moved into the -80 degrees Celsius freezer before being sliced on the cryostat.

2.5 Masson's Trichrome Staining

After taking the desired slides out of the freezer, we waited for them to defrost before they were placed in Bouin's Fixative for 20 minutes under the hood. Once the 20 minutes passed, the slides were rinsed under cold deionized (DI) water for 5 minutes until the yellow color from the Bouin's was removed from the tissues. Next, the slides were stained for 5 minutes in Wiegert's Iron Hematoxylin for 5 seconds, and then promptly rinsed under cold DI water for 2 minutes. After this rinse, the slides were stained for 15 seconds in Biebrich Scarlett- acid Fuchsin Solution and then rinsed under cold DI water until the water running off the slides was clear. The slides were then placed on the bench and 400 µL of phosphotungstic/phosphomolybdic acid was pipetted directly onto the tissues. The slides sat for 10 minutes, and the acid was discarded via a kimwipe. Next, the slides were stained in Aniline Blue for 30 seconds and rinsed 3 times for 30 seconds each in cold DI water. Then, the slides were placed on the bench again and 500 µL of Acetic Acid was pipetted onto the tissue sections for one minute. The Acetic Acid was discarded in a DI water rinse. The slides were then placed in 95% ethanol, 100% ethanol, and xylene for 2 minutes each. The final step of this protocol was mounting the slides with 55 µL of Permount.

2.6 Immunofluorescence Staining

After taking the prepared slides of a C57BL/6J mouse salivary gland, prepared by Amber Altrieth, from a -80°C freezer, they were placed in 4% paraformaldehyde (PFA) for 18 minutes. Once the 18 minutes was completed, the slides were washed two times for three minutes each in a 1xPhosphate Buffered Saline (PBS) solution. Following the washes, the slides were placed into 0.5% tx-100 (triton-x 100) solution for 18 minutes, and then washed two more times in 1xPBS. The slides were then dried with a Kim wipe, and the tissue samples were encircled using a hydrophobic pen. The wax from the pen dried, and we added blocking solution (3% Bovine

Serum Albumin (BSA), 0.5% tween-20 solution in 1xPBS) to the samples and let them sit in a pipette box partially filled with 1XPBS to make a humidified chamber for one hour. Once the hour was up, the primary antibody solution was added.

For the slides stained in chapter 3 experiment 1, of the C57BL/6J mice, the primary antibody (Ab) solution was 600 µL total and contained 3µL of rat CD31 (1:200 dilution), 1.5 µL of rabbit AQP5 (1:400 dilution) and 595.5 µL of 3% BSA. This primary solution was pipetted onto the slides, and then left to sit overnight in a 4°C refrigerator in a humidified chamber. After sitting overnight, we then washed the slides four times in 1xPBS solution for 3 minutes each. The slides where then placed in 1xPBS and let to sit in the fridge for another 24 hours. For the next steps, the slides were kept covered and out of direct contact with light. The next day, the secondary solution was then added. The secondary solution contained 1.2µL of ∝ rabbit Cy2 to detect AQP5, 1.2µL of ∝ rat no mouse Cy5 to detect CD31, 6.0 µL of ConA lectin and 591.6 µL of 3% BSA 0.5% tx-100. The secondary solution was pipetted onto the slides in volumes of approximately 150µL and let to sit for one hour, covered from the light. After one hour, the slides were washed in 1xPBS two times for three minutes. Then the slides were placed in a 4′,6-diamidino-2-phenylindole (DAPI) solution (1 µg/mL) to label nuclei for 10 minutes followed by two more washes in 1xPBS for three minutes. The slides were then dried carefully with a Kim wipe and mounted with glycerol-based mounting media (GE). Then the slides were imaged on an IX-71 Olympus microscope.

For the slides stained in chapter 3 experiment 2, of the C57BL/6J mice, the antibody solutions were made via the dilution factors indicated in **Table 1**. This primary solution containing rabbit Ki67 and rat CD31 was pipetted onto the slides, 125 µL per slide, and then left to sit overnight in a 4°C refrigerator in a humidified chamber. After sitting overnight, we then

washed the slides four times in 1xPBS solution for 5 minutes each. For the next steps, the slides were kept covered and out of direct contact with light. The secondary solution, containing ∝ rabbit Cy5 to stain for Ki67 and ∝ rat no mouse Cy3 to stain for ECs was pipetted onto the slides,125 µL per slide, and left to sit for 1 hour. The slides were then washed two times in 1xPBS solution for 5 minutes each. The slides were stored in the final 1xPBS wash and let to sit in at 4C for another 24 hours with parafilm around the lid. Then the direct conjugate containing EpCam-FITC solution was pipetted onto the slides, 125 µL per slide and left for 1 hour. After an hour, the slides were washed two times in 1xPBS solution for 3 minutes each. Then the slides were placed in a 4′,6-diamidino-2-phenylindole (DAPI) solution (1 µg/mL) to label nuclei for 10 minutes followed by two more washes in 1xPBS for three minutes. The slides were then dried carefully with a Kim wipe and mounted with glycerol-based mounting media (GE). Then the slides were imaged on a Zeiss CellObserver microscope.

Table 1

Immunohistochemistry Antibody Information

	Antibody	**Company**	**Cat Number**	**Lot Number**	**Dilution Factor**
Primaries	Rb mAb to Ki67	abcam	ab16667	GR196539-2	1:100
	Rat anti mouse Cd31	BD pharmingen	553370	7257819	1:200
Secondaries	anti-rat no mouse-Cy3	Jackson ImunoResearch	712-166-153	139421	1:500
	anti-rabbit Cy5	Jackson ImunoResearch	711-606-152	125599	1:500
Direct Conjugate	EpCAM-FITC	Invitrogen by Thermo Fisher Scientific	11-579182	2028653	1:400

2.7 Trichrome Image Quantification

The trichrome images were captured on a Lecia scope under 5x magnification. Once all of the images were acquired, Adobe Photoshop version 12 was used to stitch together each gland in order to create a whole image. In Photoshop, the automate photo-merge option was selected, and then all of the images for one tissue section were selected. The program then stitched together all of the images by observing the overlap between images. Once a whole tissue section was stitched together the image was saved as a tagged image file format (TIF) file.

All stitched trichrome images were quantified using FIJI image software. For the trichrome images the Fiji editor was opened, and the desired image was opened onto Fiji. The color threshold was then adjusted to capture the blue ECM stain: the Hue was set to 127-168, the saturation was set to 50-255 and the brightness was set to 30-255. All slides imaged on the same day, had the same settings in order to allow for accurate quantification. For outliers, the hue was adjusted differentially to determine if we could accurately measure trichrome area and is indicated as such. Once this threshold level was set, and the area of trichrome was selected, a mask was created. The mask shows only the area of highlighted trichome in white, against a black screen. The measure function was then used to measure the amount of trichrome on the mask. Then, the freehand select tool was used to draw an outline around the original tissue image. A new region of interest (ROI) was created and then the manager function was used to measure the total amount of gland area in the image. All of the quantifications were compiled in excel.

2.8 IHC Image Quantification

All of the chapter 3, experiment 1 IHC slides were imaged on an Olympus IX-71 microscope with a Peltier-cooled CCD camera (Q imaging, RET 4000DC-F-M-12) using a PLAN S-APO 20X, 0.75 NA objective, and all of the chapter 3 experiment 2 IHC slides were imaged on Zeiss Z1 Cell Observer widefield with an Axio712 mono camera using a "Plan-Neofluar" 20X/0.50 Ph2 M27 objective. The images collected from both scopes were opened into the Fiji editor software and the background was subtracted. Once these adjustments were made, the threshold was adjusted and verified using the create selection tool. A mask was then created and analyzed using the set measurement tool. The measurement allows for the area selected for in the threshold to be measured. For each day that slides were imaged, the threshold was set to the same level for each channel. To determine the total tissue area, the Ep-Cam-FITC channel was used, with no background subtraction, and a threshold was picked so that the entire tissue section was selected. This threshold was used for all of the sections imaged on one day, and each day had its own threshold. Once all channels for one tissue section were adjusted and imaged, the four channels, DAPI, EpCam-FITC, CD31 and Ki67 were merged together to create a composite image. All channels were then normalized to DAPI or the total tissue area by dividing the channel area by DAPI or total tissue area.

2.9 Statistical Analysis

All tabulation of quantification was performed in Microsoft Excel. Sections with low tissue quality due to poor fixation or tissue loss were excluded from quantification. For studies with only two conditions, an unpaired two-tailed t-test was performed using GraphPad Prism version 9.1.2 for Windows, GraphPad Software, San Diego, California USA, www.graphpad.com. For studies with more than two conditions, an Ordinary one-way ANOVA

with Tukey multiple comparisons analysis was performed using GraphPad Prism. Analysis containing statistically significant results are indicated by stars over the corresponding bars and the p values are listed in the figure legends. Analyses with no statistical significance ($p < 0.05$) are left unmarked.

Chapter 3: When do Endothelial Cells Contribute to Recovery from Salivary Gland Fibrotic Injury?

3.1 Introduction

Endothelial cells (ECs) are cells that are found lining the blood vessels and as seen in previous studies, have been deemed a requirement for the epithelial patterning of the salivary gland created during the process of vasculogenesis (Kwon et al., 2017). ECs are also important in the growth of many tissues through the secretion of paracrine acting factors, including growth factors, cytokines, chemokines, and ECM components called angiocrine factors (Rafii et al., 2016). Angiocrine factors are found within the ECs and have been shown to aid the organ repair from injury. ECs are important during regeneration of many organs and have been shown to change in response to injury. Angiocrine factors have been shown to be tissue specific (Ding et al., 2010) and to change in response to different types of injury (Rafii, 2016). No previous studies have looked into angiocrine factor production in the salivary gland or the impact of ECs on salivary gland regeneration.

To study mechanisms through which glands can recover from injury, the salivary gland ductal ligation model has been developed (Woods et al., 2015). During the process of ligation, a clip is placed on the main ducts of the submandibular (SMG) and sublingual gland (SLG) which leads from the salivary glands to the mouth. The main excretory duct of the SMG is Wharton's duct, and the main excretory duct of the SLG is the Bartholin's duct. These two excretory ducts meet and connect at the sublingual caruncula (Holmber & Hoffman, 2014). During ligation, extracellular matrix deposition (ECM) increases. Excess ECM deposition can result in fibrosis, which can be detected by Masson's trichrome stain. Ligation causes a reversible fibrosis injury that affects gland function. With fibrosis, the gland begins to atrophy or waste away, and acinar

cell loss occurs. Acinar cells are defined as any cell that lines an acinus, which is a small sac-like cavity in a gland surrounded by secretory cells, and these cells have been known to decrease after ligation. The longer the clip is held in the place during ligation, the smaller and less productive the salivary gland will become.

Deligation is the removal of the clip placed on the duct. Based off previous research, following deligation, acinar cells can fully recover following deligation (Cotroneo, 2008). This data is based off saliva samples, as saliva can only be produced if acinar cells are functional. During deligation, the level of functional acini in the salivary gland will begin to increase and the amount of cell inflammation and fibrosis decreases. Previous work demonstrated that the amount of trichrome staining decreases after deligation. However, these studies have not looked at the endothelial cells and when they begin proliferating during the repair process.

The main purpose of our research is to determine how the salivary glands can regenerate following trauma, and how this can be useful in developing therapeutics for treatments of diseases like SS. Current treatments for hyposalivation are only palliative, and so the discovery of new regenerative therapies is needed. We want to examine two main topics throughout this research; the first component that we would like to determine is the timing of the decrease in ECM relative to the increase in acinar cells following deligation. We also want to determine how endothelial cells may contribute to recovery following deligation. I would hypothesize that once the vasculature clip is removed, the increased presence of pro-regenerative angiocrine factors should aid in the regeneration of salivary glands. In our study, we will be able to determine to what extent the level of endothelial cells increase by quantifying the number of CD31-positive cells present in the glands and when they are proliferative by counting the number of Ki67+, CD31+ cells in salivary glands that have been ligated compared to gland that have gone through

delegation. We will identify the timepoint when the endothelial cells start to proliferate as we will identify angiocrine factors from ECs just prior to cell proliferation in future studies.

3.2 Methods

All methods used in this chapter are explained in chapter 2 of this paper. The methods used for this set of experiment were mouse breeding and husbandry, ductal ligation and deligation surgery, Masson's trichrome staining, immunofluorescence staining, and statistical analysis.

3.3 Results

Experiment 1:

Ductal ligation surgeries were performed on the left glands of 12-week-old female C57BL/6 mice which were prepared for cryosectioning and IHC. Some of the glands were harvested without removing the clips (ligated control) and on some the clips were removed and the glands were allowed to regenerate (delegated). These glands were compared to time zero mice in which the SMGs were harvested at the time of surgery and mock surgery. Slides from C57BL/6 mice were stained and imaged. Four of the slides were used as a control, meaning that the gland was harvested from a 3-day mock surgery where the ducts corresponding to the SMG gland were not ligated. The meaning of this control was getting a baseline of where each cell level is at prior to injury and eliminating any effects of the surgical manipulation itself. The other 5 slides were of 3-day deligated tissue, which were obtained from glands three days after removal of the clip. For the T0 mouse there were 6 slides used and the 14-day ligated tissue had a sample size of 8.

When completing the immunofluorescence staining, we stained for acinar cells via the staining of glycoproteins and glycolipids, concanavalin A (ConA), and AQP5, endothelial cells

via CD31, and DAPI, which labels the cell nuclei. AQP5 was detected with a Cy2 conjugated secondary antibody and is important to this study as it stains for the water channel proteins, and therefore indicates where the acinar cells are. ConA was detected with a Cy3 secondary antibody and stains for glycoproteins and glycolipids present within the saliva, and therefore also indicates where the acinar cells are located and if they are producing glycoproteins and glycolipids. CD31 was detected with a Cy5 conjugated secondary antibody and is a cell surface receptor on endothelial cells within blood vessels; and DAPI stains for cell nuclei. These stains allow for us to determine if the cells in the salivary gland are beginning to regenerate or if there are still in an injured, fibrotic state. Immunofluorescence staining was used to stain certain cell markers and the FIJI software system was used to quantify the data. We used a lectin, conavalinA (ConA), which comes from the jack bean and binds to glycoproteins, which was conjugated to a fluorophore and exposed it to tissue sections obtained from deligated and mock surgery control glands to examine levels of glycoproteins in glands 3 days after deligation. **Figure 2A** shows a composite image from the apical side of a 14-day ligated surgery mouse identified as L1. **Figure 2B** shows a composite image from the distal region of the gland of a deligated C57BL/6 mouse, identified as R1L2. The gray color is representative of DAPI, which stained the nucleus of each cell. The magenta color is representative of ConA and stains the glycoproteins and glycolipids present the in saliva. The deligated slide has tissue that was ligated for 14 days and deligated for 3 days prior to harvest.

Figure 2

ConA detection of glycoproteins in deligated salivary glands

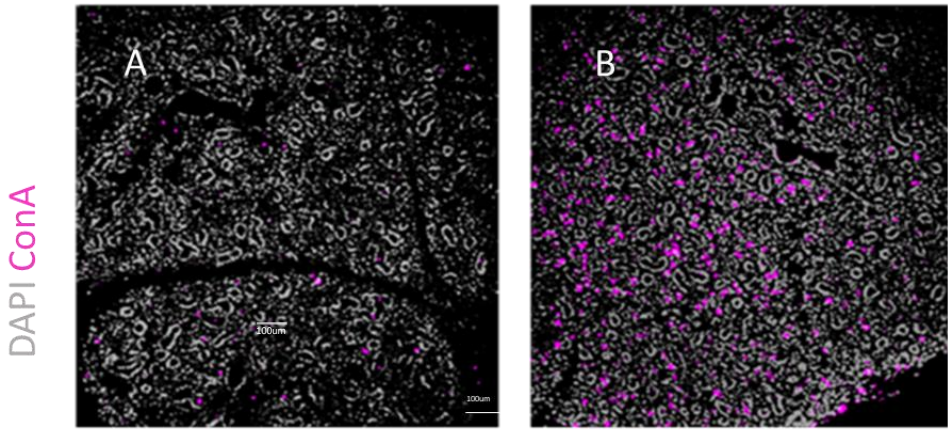

Note: We used a lectin, conavalin (ConA), which was conjugated to a fluorophore, and exposed it to tissue sections obtained from deligated and mock surgery control glands to examine levels of glycoproteins in glands 3 days after deligation. ConA Lectin is magenta and DAPI (gray), stains for the cell nuclei. **Figure 2A** is the 14-day ligated gland tissue and **Figure 2B** is the 3 day deligated tissue.

As a complementary method to examine the acinar cell recovery, we performed IHC to detect the water channel protein, aquaporin 5. We exposed the deligated and control tissues to an antibody to detect AQP5 (green) followed by a secondary antibody conjugated to a fluorophore. the gray stain is DAPI, and that stains for the cell nuclei. In **Figure 3**, we stained for AQP5 to demark acinar cells within the SMG gland. **Figure 3A**, is composite image from the apical side of a deligated C57 mouse with the identity of R1L1. This slide was ligated for a period of 14 days and then deligated for 3. **Figure 3B** is a composite image from the apical side of a 3-day mock C57 mouse identified as R1. After we finished imaging our IHC images using FIJI, we were able to quantify the areas of each stain relative to the stain for DAPI. **Figure 3C** illustrates the quantifications for the AQP5 stain normalized to DAPI. The deligated tissue has 0.8-fold less AQP5 positive area when compared to the mock control but more than the delegated glands. The T-test that we ran yielded a value of 0.45, which means the difference is non-significant.

Figure 3

AQP levels in deligated salivary glands.

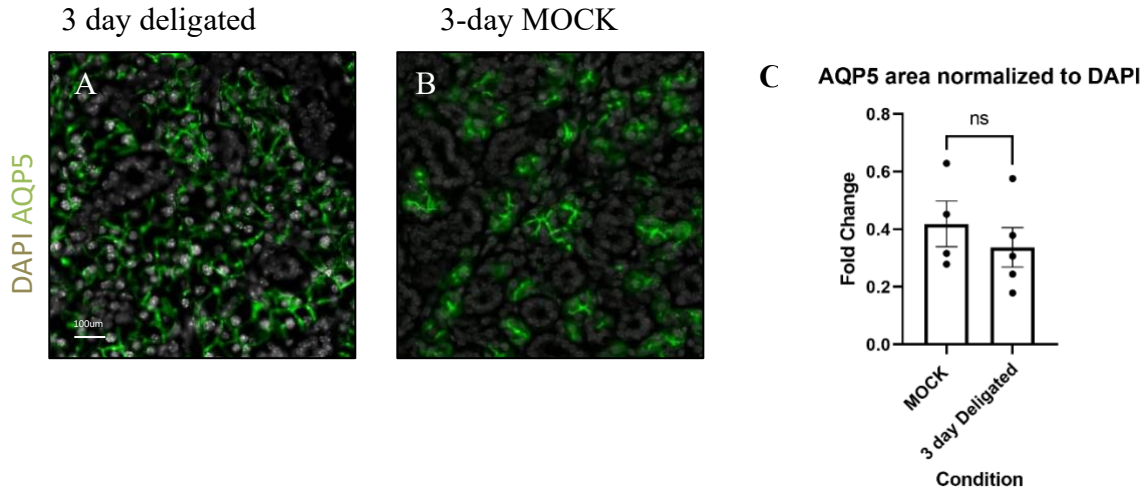

Note: **Figure 3A** shows 3 day deligated gland tissue and **Figure 3B** shows 3-day mock gland tissue. IHC was performed to detect AQP5 (green) and DAPI (gray). **Figure 3C** the area positive for AQP5 was quantified relative to the area positive for the nuclear stain, DAPI. We expressed the AQP5/DAPI area levels as a fold change relative to the mock tissue. The error bars correspond to S.E.M. n=4 for the mock and n=5 for the deligated tissue.

In addition to staining for acinar cells using ConA and AQP5, saliva measurements are another way to monitor salivary gland recovery. We wanted to determine if stimulated saliva measurements could be used to determine successful ligation upstream of deligation surgery. Saliva was collected at 1, 2, 4, and 6 weeks to determine how injury impacts the acinar cells. Weeks 1, 2, and 4 provide us with the baseline data and week 6 was one week after surgery. If the acinar cells are injured, less saliva should be produced. We induced saliva production in 15 C57 female mice using pilocarpine prior to injury and post-surgery to observe what the effect of ligation is on the production and secretion of saliva. In **Figure 4A**, saliva weights for weeks 1, 2 and 4 were averaged together to create the before surgery saliva weight. Week 6 saliva weight was measured 1 week after ligation surgery. All of the saliva weights were then normalized to mouse weight (NMW). After the mice were harvested, the glands were weighted and a cut off was created to define which glands had successful ligation. The cutoff range was between 0.019

and 0.044g, and any left gland that fell within this range was considered a successful ligation. Only the left gland was examined, as we only ligated one gland. The mice that appeared to have a successful ligation were, R1, R2, R2L1, R2L2 and R3, with left gland weights of 0.035g, 0.033g, 0.029g, 0.031g, and 0.027g respectively. These glands were marked with an asterisk in **Figure 4A**. There was no trend between successful ligation and lower saliva production, and this can be seen in **Figure 4B**.

Figure 4

Quantification of Saliva production before and after ligation surgery

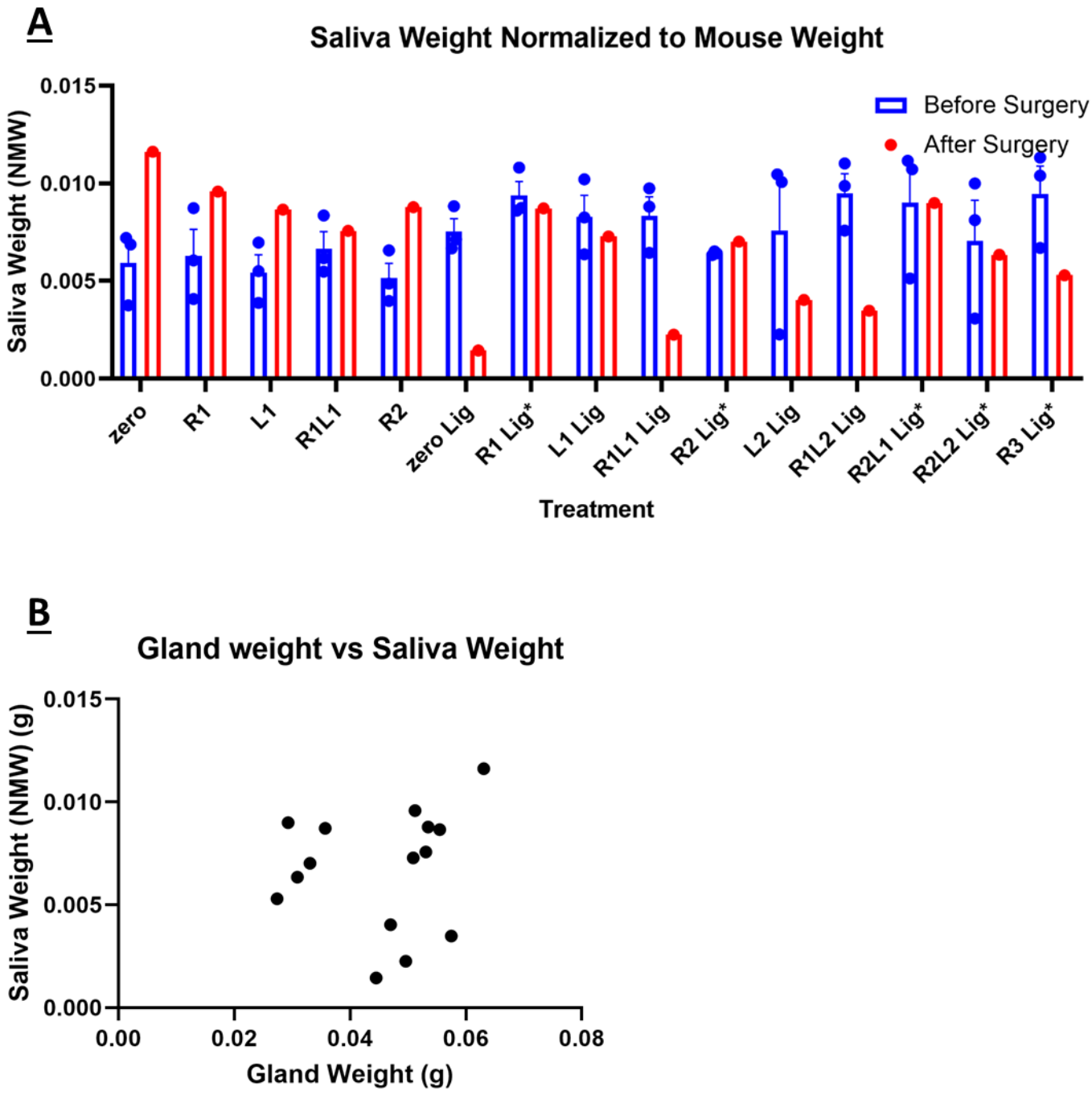

Note: After following the saliva collection protocol, saliva was collected during weeks 1, 2, and 4 leading up to ligation surgery, and one week post ligation surgery, week 6. In Figure 4A all of the weights were then normalized to mouse weight. The first four mice were used as controls, and not ligated. The mice identifications with asterisks in the name, are considered to have successful ligation surgeries. Figure 4B, shows the correlation between successful ligation, which was determined by gland weight and saliva weight.

After comparing multiple methods for assessing salivary gland function, we next focused on the endothelial cells, which may promote salivary gland regeneration after deligation. To examine endothelial cells in the blood vessels, we preformed IHC to detect CD31, a cell surface marker that expressed by endothelial cells. We compared the gland before injury (T0), after 14 days ligation, after 14 days ligation with 3 days deligation, relative to a 3-day day delegation mock surgery. In **Figure 5**, we used CD31, as shown in red, to stain for the endothelial cells in the SMG. CD31 is a cell surface marker that expressed by endothelial cells. The grey stain shown in these images is DAPI, or the nuclear stain. **Figure 5A** is the gland at T0, this tissue was not exposed to any injury and allows us to determine the level of ECs in a healthy, normal, salivary gland. **Figure 5B** is the SMG directly following the 14-day ligation. This tissue indicates the levels of ECs in a fibrotic, injured gland. **Figure 5C** is the 3-day mock tissue, and this mouse was not ligated at all, however it did undergo two rounds of exploratory surgery, in which the salivary gland and its corresponding ducts were located but not ligated or deligated. This tissue was from the apical side of the R1L1 C57 female mouse. **Figure 5D** is the 3-day deligated SMG tissue, and this image allows us to get a glimpse into what the gland is beginning to do following the removal of the source of injury. This tissue was from the apical side of the R1 C57 female mouse.

Figure 5

Endothelial cells in injured and control salivary glands

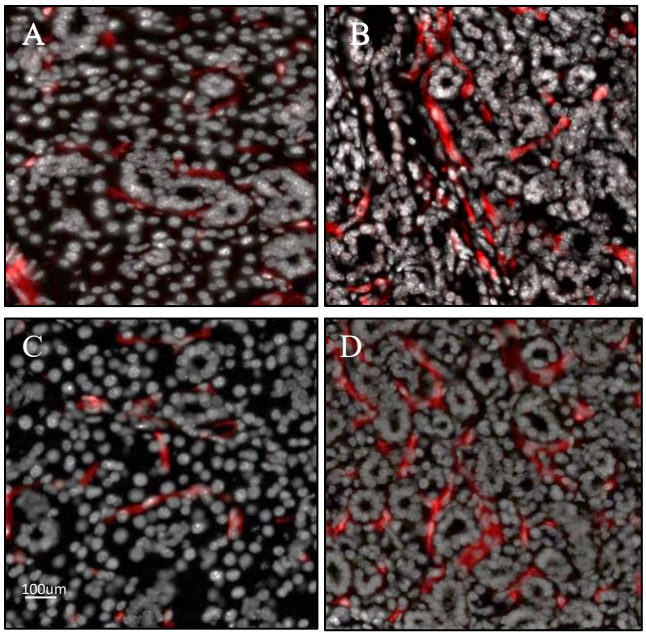

Note: To examine endothelial cells in the blood vessels, we preformed IHC, to detect CD31(red) and DAPI (gray) for cell nuclei. We compared the gland before injury at T0 (**Figure 5A**), after 14 days ligation (**Figure 5B**). We next compared the 3-day mock tissue (**Figure 5C**) and 3-deligated tissue (**Figure 5D**).

We compared the gland before injury (T0) and after 14 days ligation and saw that the endothelial cells present increased by more than 2-fold by quantifying the area positive for CD31 relative to DAPI. We next compared the deligated tissue and found that it has 1.5-fold more CD31 stain than the mock. The trend shown is that the ECs are increasing with ligation and remaining present after deligation. **Figure 6** illustrates the quantifications for the value of positive CD31 stain relative to DAPI. The trend that can be seen is that the ECs are increasing following ligation and remaining relatively high 3-days after deligation. We ran a one-way ANOVA test which yielded the differences between each of our values as non-significant, expect for the difference between the 3-day mock and 14-day ligated samples; suggesting that the ECs

are increasing with injury, but the endothelial cell area does not expand significantly after deligation.

Figure 6

Quantification of CD31 in ligated and deligated salivary glands.

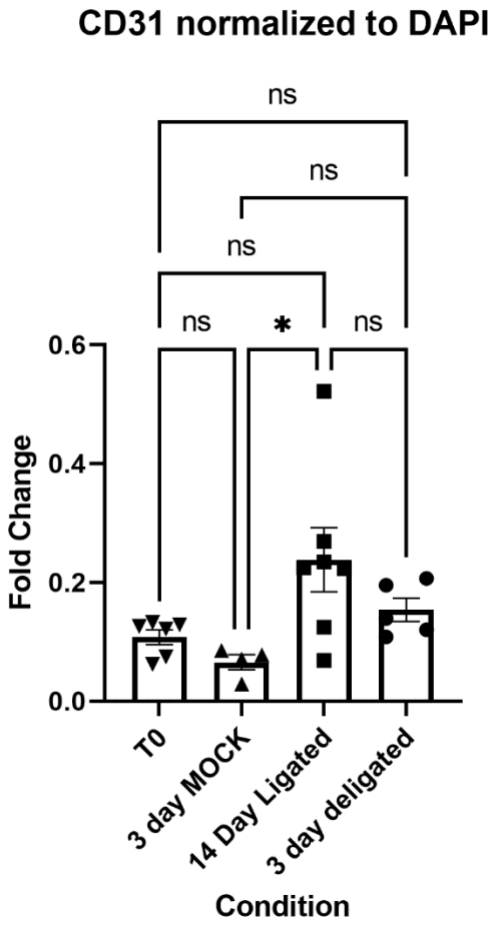

Note: After preforming IHC on 3-day mock and 3 day deligated tissue, we were able to quantify the area positive for CD31 relative to the area positive for the nuclear stain, DAPI. We expressed the CD31 area levels as a fold change relative to the mock tissue. The 14- day ligated tissue was harvested before the gland was deligated, and the T0 tissue was harvested prior to any induction of injury. The error bars correspond to S.E.M.

Experiment 2:

To compare the extent of the fibrotic response following delegation, we performed a ligation surgery for 2 weeks followed by a delegation for either three days or seven days and compared the extent of ECM deposition by trichrome staining. 41 slides, containing tissue from 41 C57 female mice were selected for this trichrome experiment. There were 15 slides, with a sample size of 30 salivary gland tissues for the 3 day deligated condition. There were 7 slides, with a sample size of 20 salivary gland tissues for the 7 day deligated. There were 5 slides, with a sample size of 5 for the 14 ligated condition. For the 3-day Mock condition, there were 9 slides, with a sample size of 18 salivary gland tissue section and lastly, for the 7-day Mock condition there were 5 slides, with a sample size of 15 tissue samples. In **figure 7A** one representative tissue section from each experimental condition is shown. These tissue sections were all stained using Mason's trichrome. Trichrome staining was quantified using ImageJ. Below each stitched trichrome image in this figure, there is a mask highlighting the area of the tissue that was identified as ECM. In quantifications, the masks are used to ensure that we are measuring the correct amount of ECM, with little to no background. **Figure 7B** is a graph depicting the average trichrome, or ECM, area across all of the conditions. The average trichrome area is a percent, pertaining to the amount of ECM divided by the total tissue area. The 3-day mock condition has an average trichome area of 5.6 percent compared to the total tissue area. The 7-day mock condition has an average trichome area of 5.9 percent of the total tissue area. The 14-day ligated sample has an average trichrome area of 18.1 percent of the total tissue area. The 3 day deligated sample has an average trichome area of 9.5 percent of the total tissue area and the 7 day deligated sample has an average trichome area of 12.1 percent of total tissue area. The differences between the two mock conditions were not significant and the differences

between the two deligated condition is not significant. But the difference between the each of the mock conditions and each of the deligated conditions is significant when compared to the 14-day ligated sample. In **Figure 7C** there is an example of a representative mask, which is picking up primarily ECM staining. This tissue is the 3 day deligated sample as seen in **Figure 7A,** and as shown, the mask is correctly highlighting the amount of ECM present in the cell. **Figure 7D** indicates a trichrome sample that did not allow for proper ECM definition. The trichrome stain itself appears to be overly blue, which can be further confirmed by the mask that captures most of the tissue. Since the tissue color itself is too close to the ECM color after trichrome stained, the software is unable to distinguish the area of tissue positive for ECM when compared to the total tissue area. This is why the mask appears to be a mask of the whole tissue. This image was deemed to be an outlier and was not included in the quantification.

Of the 41 slides stained for ECM with trichrome in **Figure 7A-C**, there were tissue sections from surgeries performed by two different researchers, Amber Altrieth, and Dr. Kevin O'Keefe. To determine if the surgical technique by the two researchers was equivalent, we compared gland size and trichrome staining. After the glands were harvested, the weights were compared and found to be similar (data not shown). Trichrome staining was also compared. In **Figure 7E** the three day deligated and three-day mock tissue sections were compared from these two researchers in order to determine if the two surgeon's samples could be combined with one another. Although the mock surgery results were the most variable, there was no significant difference between the trichrome staining results from the surgeries performed by the two researchers, indicating that all of the surgical data could be compared in the same experiment. Due to not having any 7-day data to compare Dr. Kevin O'Keefe vs Amber Altrieth, data, we choose to stay with solely Amber's surgery glands in subsequent figures.

Figure 7

Trichrome quantifications of C57 mice

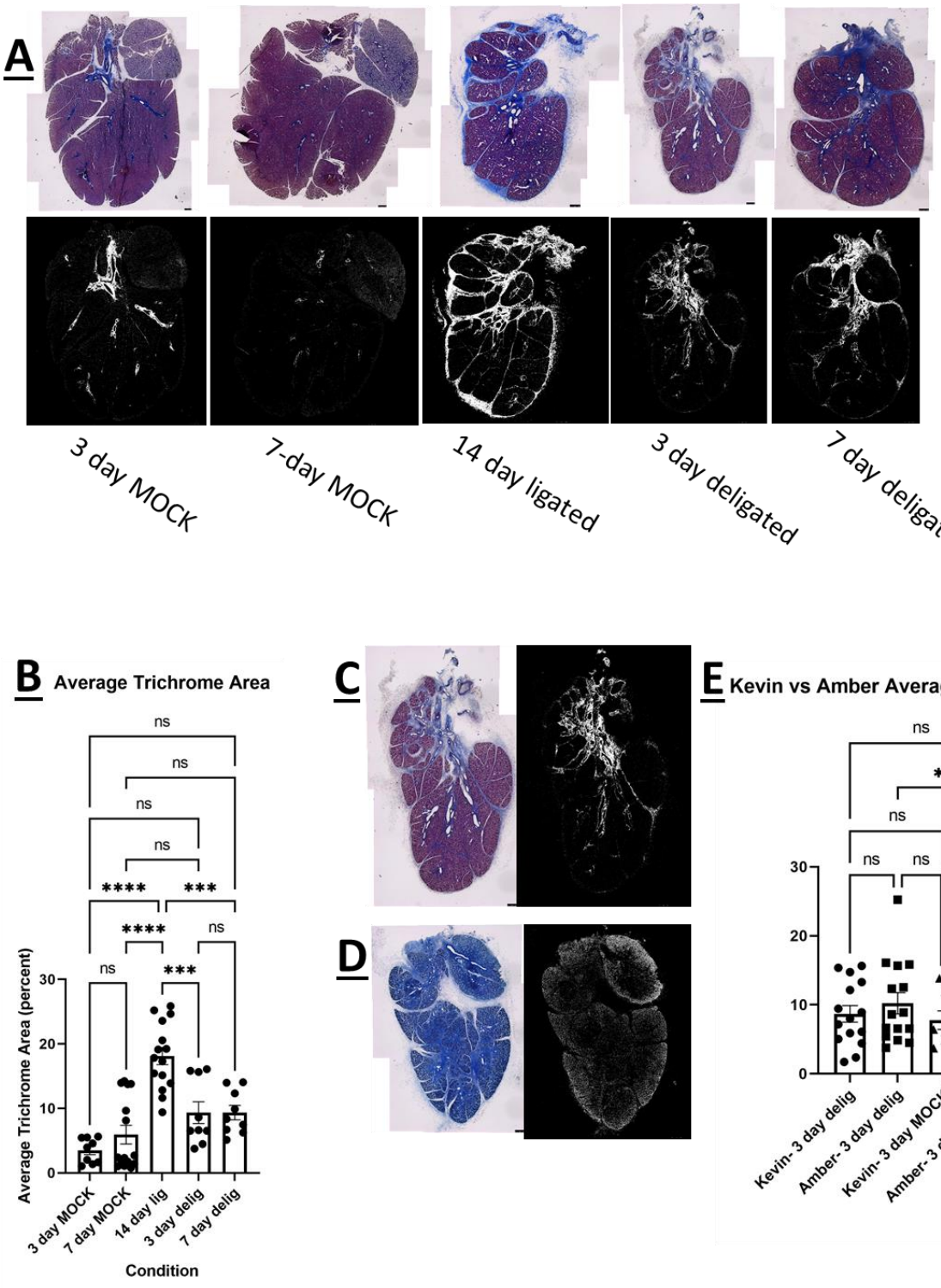

Note: In **Figure 7A** there is a stitched Trichrome image of each condition with its corresponding mask under it. We measure the amount of Trichrome from an image. When the staining is done correctly, the trichrome will end up becoming a dark blue color, whereas the rest of the tissue will remain a pink color. This allows for us to use NIH Imaging software to select all of the blue colored trichrome, which can be seen in the mask. **Figure 7B** is a graph of the Trichrome quantifications for each condition. Each condition is on the x-axis and the average trichrome area is on the y-axis. A one-way ANOVA test was used to obtain the significance. **Figure 7C** is a depiction of a correct mask. The tissue was correctly stained, and the mask correctly indicates the trichrome area. **Figure 7D** shows what happens when something goes wrong with the staining. As seen in the colored image, it is difficult to distinguish the trichrome from the remaining tissue. As much as we have an issue with distinguishing the tissue, the programing software has the same issue. The software cannot tell the difference between the trichome and other tissue, and therefore selects it all, which can be seen in the mask. Tissue sections that showed a pattern similar to this were excluded from our calculations, as they are inaccurate and over-select the trichrome area. **Figure 7E** shows the comparison between two different researchers' 3 day deligated and MOCK surgeries.

When conducting the immunohistochemistry staining for this experiment, we stained for DAPI, EpCam-FITC, CD31, and Ki67. DAPI stains for the cell nucleus and allows us to visualize each cell. CD31 is in the Cy5 stain and is a cell surface receptor on endothelial cells blood vessels and stains for them. EpCam-FITC is in the Cy2 stain and is an is a cell surface receptor on epithelial cells; and Ki67 is a cell proliferation marker in the Cy3 stain. These stains allow for us to determine at what stage the salivary gland cells are beginning to proliferate. Immunofluorescence staining was used to stain certain cell markers and the FIJI software system was used to analyze the data. Over the course of 5 days, 20 slides from C57 mice were stained and imaged. 3 of the slides were used as a control, meaning that the gland was harvested form a 3-day mock surgery, and the ducts corresponding to the SMG gland were not ligated. The meaning of this control was getting a baseline of where each cell level is at prior to injury. The other 17 slides were of 3-day deligated tissue, 7 day deligated, and 14-day ligated tissue. In **Figure 8A** the IHC images from each condition are shown. Within each condition there is an image of DAPI with EpCam-FITC, DAPI with CD31, DAPI with Ki67 and a composite of all stains. **Figure 8B** is a graph of the area of EpCam-FITC positive stain over total tissue area for each tissue. The EpCam-FITC area average normalized to total tissue area are 0.261, 0.220, 0.230, 0.200 for the 3-day mock, 14 days ligated, 3 day deligated and 7 day deligated

respectively In **Figure 8C** there is a graph indicating the CD31 positive area over the total tissue area. The CD31 area average normalized to total tissue area are 0.029, 0.090, 0.043, 0.096, for the 3-day mock, 14-day ligated, 3 day deligated and 7 day deligated respectively. In **Figure 8D** there is a graph of the Ki67 positive area over the total tissue area. The Ki67 average area normalized to total tissue area are 0.005, 0.015, 0.049, and 0.012 for 3-day mock, 14-day ligated, 3 day deligated and 7 day deligated respectively. In **Figure 8E** the quantitation of DAPI area over total tissue area is shown for each condition. The DAPI areas normalized to total tissue area are 0.257, 0.436, 0.300,0.355 for the 3-day mock, 14 days ligated, 3 day deligated and 7 day deligated respectively A one-way ANOVA test was used with these all of these quantifications in order to obtain the significance between conditions. Although we do not have any significant changes in our data, we can observe that EpCam-FITC levels remain constant across all conditions, and that CD31 levels are increasing when the tissue is injured, 14-day ligation, decrease at the 3-day deligation and increase at 7 day-deligation; both of which has been shown in previous research. The Ki67 positive stain is relatively low at the 3-day mock and 14 ligation timepoints, which is what previous literature has suggested, and peaks at the 3-day deligation timepoint. Lastly, the DAPI stain stays constant across all conditions, which is what is expected. These findings suggest that we should examine between 3- and 7-days post deligation.

Figure 8

Immunohistochemistry of C57 mice between various conditions

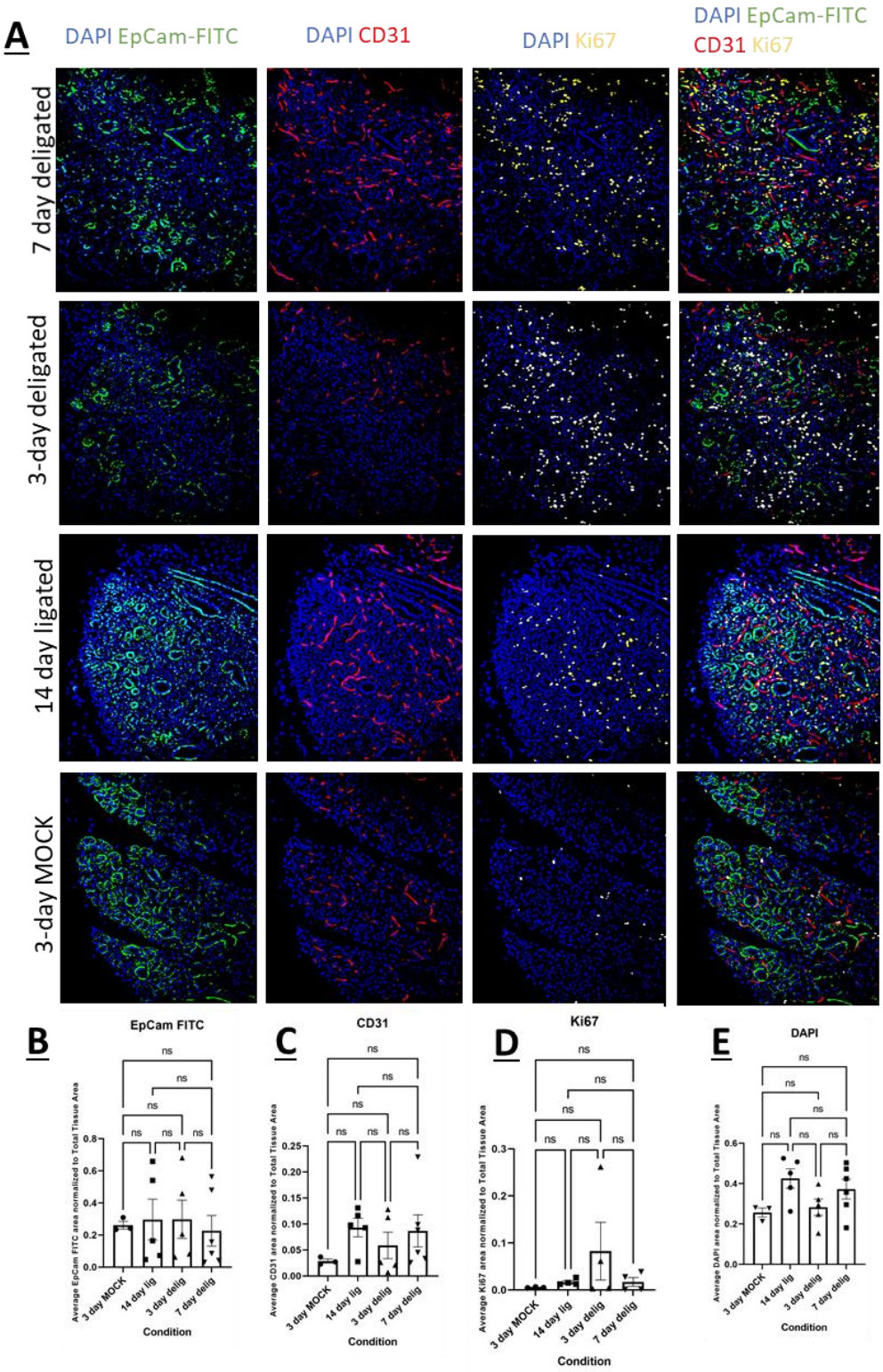

Note: In **Figure 8A** IHC images are shown for each of the following conditions: 3-day MOCK, 14 days ligated, 3 day deligated and 7 day deligated. For each condition there is an image of DAPI with EpCam-FITC, DAPI with CD31, DAPI with Ki67 and a composite with all of the stains. This allows us to visualize how the stains are fluctuating between each condition. **Figure 8B** is a graph of the EpCam-FITC positive area was normalized to the total tissue area. In **Figure 8C** the area positive CD31 was quantified and normalized to the total tissue area. **Figure 8D** is a graph of the Ki67 positive area normalized to the total tissue area. In **Figure 8E** the DAPI positive area normalized to the total tissue area was quantified for each condition. The statistics for **figures 8B-E** were ran with a one-way ANOVA test

3.4 Discussion

Experiment 1:

Throughout IHC staining and saliva collections we were able to state what happens to the SMG gland when injured. We used the ductal ligation-deligation model to induce a reversible injury in the mice, and after 14 days of ligation, we removed the clip. The days following deligation, we were able to observe how, or if, the SMG gland was beginning to recover. We focused specifically on acinar and endothelial cells in our IHC. Our results indicate that at 3-days, the acinar cells are not expanding, and the endothelial cell levels are still high. This suggests that the salivary gland is not yet beginning to recover, as there is still inflammation present (high EC positive tissue).

Our first method in examining the SMG was IHC. We did a total of three different stains, two for acinar cell markers and one for ECs. In **Figures 2, 3 and 5**, the immunofluorescence staining protocol was used to stain certain cell markers. This was done on C57BL/6 mice to observe how the cells within the SMG gland respond to injury. In **Figure 2,** the ConA stain is shown. As seen by the images, the 3-day deligated tissue (**Figure 2B**) has the most ConA positive area, compared to the 14-day ligated (**Figure 2A**) conditions. We were not able to quantify this stain, but the amount of ConA appears to increase following deligation.

The second acinar cell marker that we examined via IHC was AQP5. In **Figure 3,** there is more AQP5 staining in the deligated tissue (**Figure 3A**), when compared to the mock tissue

(**Figure 3B**), indicating that the acinar cells have not fully recovered following ligation. In **Figure 3C** we were able to quantify the areas positive for AQP5. **Figure 3C** depicts the area positive for AQP5 relative to DAPI and as shown, there is more positive area of AQP5 in the mock tissue when compared to the deligated, which indicates that the acinar cells have not fully recovered 3 days after deligation. The difference between the deligated and mock tissue areas positive for AQP5 were not significant according to our T-Test. This could be do a low sample size of 4 mock and 5 deligated glands and could also be due to high variability, as we have one sample in each condition that have very high levels; so, a larger sample size could allow us to see if our values are significant given the level of variability. If the SMG was beginning to recover, we would begin to see the acinar cell levels return to control/mock levels; however, that is not what we observed meaning that at 3 days. The acinar cells in the gland are not recovering at 3 days. However, previous research done by Cotroneo in 2008 on rats concludes that 3-days after deligation the morphological traits, such as acinar cells, begin to return in the SMG. Although our findings do not match these findings and that could be due to difference in recovery times between the two types of animals, our findings were not significant. Once, we increase our n-value, for these experiments, we will be able to more accurately state how our findings relate to past research.

To examine how injury impacts the SMG in a broader sense, we performed a saliva collection on mice pre- and post-ligation. In **Figure 4A**, the saliva weight collection was graphed. As shown by the graph, it seems that some of the saliva production decreased following ligation; however, when we harvested the glands there was little to no change in weight, suggesting that ligation was not successful. From this data, we can conclude that pilocarpine-induced saliva measurements are not a reliable way to determine successful ligation. We are only

affecting one gland with the surgery and stimulated saliva tends to stimulate primarily the parotid gland (which is unaffected in our surgery), so this could be a major reason as to why this technique was ineffective. It is possible to canulate the submandibular gland to collect just saliva from one SMG at a time, which could be tested in future experiments (Kuriki et al., 2011). **Figure 4B** is showing the correlation between the glands that were successfully ligated, which we determined from gland weight, and saliva weight. As can be seen from the figure, there is no correlation between ligation and saliva production with this methodology.

Due the discovery that the acinar cells have not fully recovered after 3- or 7-days following ligation, we next observed the ECs since they have a known role in both inflammation, and regeneration. To examine how injury impacts the SMG, we choose to stain for CD31, which is an EC marker. In **Figure 5**, we compared the IHC staining compositions at four different time points. **Figure 5A** is the SMG tissue at T0, which means that the gland was harvested prior to any induction of injury. This image gives us a comparison of what a normal, healthy SMG gland's EC level should be. **Figure 5B**, is SMG tissue 14 days after ligation, which means that the ducts were never deligated, the glands were just harvested after ligation. This allows to us observe what the EC levels are like at the peak level of fibrosis. **Figure 5C** is from the R1, 3-day mock C57 female mouse, which means that the mouse underwent a mock surgery, and 3 days later the glands were collected. This allows us to observe what happens to the SMG gland when the mouse itself is placed under stress and injured. **Figure 5D** is from the R1L1, 3-day deligated C57 female mouse. This tissue is what we are focusing on, as this will tell us what the ECs look like after the removal of the source of injury. In **Figure 6**, we were able to quantify the areas positive for CD31. **Figure 6** depicts the area positive for CD31 relative to the area for DAPI. The number of ECs present in the 14-day deligated tissue was 2-fold higher than the T0 tissue

and the number of ECs present in the 3-day deligated tissue was 1.5-fold higher than the mock tissue. This trend indicates that the ECs are increasing with ligation and remaining high 3-days following deligation. We expect for the ECs to be high when they are activated, in times of injury or inflammation and repair. Due to the EC levels remaining high 3 days following deligation, the inflammation might still be present. The differences in the areas positive for CD31 between each time point are not significant, except for the difference between the 3-day mock and 14-day ligated samples. This insignificance could be due to the limited sample size for T0, 14-day ligated, 3-day deligated and mock which was 8, 5, 5, and 4 respectively, or due to high variability between mice. The significance between the 3-day mock and 14-day ligated samples indicates that the ligation was successful, as the increase in ECs correlates with recovery from injury.

Experiment 2:

Mason's trichrome was used to quantify the levels of ECM deposition present in each of our surgical conditions. In **Figure 7A,** one composite trichrome image from each condition was chosen, with its appropriate mask. We can observe that the 3- and 7-day MOCK tissue sections visually had the least amount of trichrome. This is what we would expect because the glands themselves were not being injured. The 14-day ligated condition seemed to have the most trichrome stain, which is also what we would expect because the gland was injured and not given any time to recover. Lastly, the 3-day 7 day deligated tissue samples were similar in the amount of trichrome visually present in the images. In order to comment on the amount of trichrome more accurately in each image, **Figure 7B** contains a graph of the average trichrome area in each condition normalized to the total tissue area. Between the 3- and 7-day MOCK conditions, there was no significant difference in trichrome area. This is what we would expect since the salivary

glands are not being injured in these two conditions. The 14-day ligated samples had the most trichrome in the images, and in the quantifications. There is a significant difference between each of the other conditions and the 14-day ligated condition suggesting that the gland is recovering and confirms that this is a reversible fibrosis since it is decreasing after deligation. For the last two conditions, the 3 and 7 day deligated samples, there was no significant difference in trichrome levels. This is also consistent with the images in **Figure 7A.** All of these findings are consistent with previous literature on fibrotic diseases; the amount of ECM will increase when the tissue is being injured, and as the tissue begins to recover the amount of ECM will begin to decrease. To better understand how we measured the amount of trichrome present in each tissue sample, **Figure 7C** is an accurate representation of an appropriately stained tissue and an appropriate mask. The mask should highlight the areas of the tissue that are blue (the ECM), and when we can correctly highlight the ECM-positive area, then we can accurately measure the correct amount of trichrome in the tissue sample. However, staining does not always work correctly, sometimes due to age or quality of the fixed tissue. **Figure 7D** is an example of a tissue sample, whose staining did not turn out as expected. This stained tissue sample ended up being overly blue, which is an issue because in the FIJI imaging software we use, it measures the amount of trichome by the amount of blue stained tissue. If the whole tissue sample is blue, as this one is, the mask will highlight the total tissue. This yields us an untrue quantification, as the whole tissue is not solely composed of ECM. We omitted all of the tissue samples, five slides, that had this issue, as it would have inaccurately represented the percent area covered by ECM deposition.

Another variable we examined while staining for trichrome was variability in samples due to different surgeons. For this comparison all of these slides were trichrome stained and

quantified in order to determine how different the surgeries were between two surgeons, Amber Altrieth, and Dr. Kevin O'Keefe. If each person performed the surgeries in a similar manner, we would expect to see no significant difference between the quantifications for the same condition. This is what we saw when we compared the data. There is no significant difference between Kevin and Amber's 3-day deligated samples, and there was no significant difference between their 3-day MOCK tissue samples either. However, after comparison of techniques, Amber and Kevin performed their mock surgeries differently and we choose to only use Amber's slides for the final trichrome quantifications. In addition, there were no 7-day mock surgery samples of Kevin's that we could use for comparison, and only Amber had a significant difference between her 3-day deligated and 3-day MOCK samples. For these reasons, we used only Amber's samples in the subsequent analysis.

We also examined the amount of different cell types of presents using immunohistochemistry. To determine when the cells in salivary glands are proliferating, we conducted IHC on 20 slides and performed IHC to detect DAPI, EpCam-FITC, CD31 and Ki67. In **Figure 8A** the 3-day MOCK, 14-day ligated, 3-day deligated and 7-day deligated conditions are shown. Within each condition, a merged image for each stain was shown, in addition to the final composite image containing all of the stains. The EpCam-FITC appears to stay consistent across all of the conditions, and the CD31 appears to increase at 14-day ligation, decrease at 3 days of deligation and then increase again. This is consistent with previous literature as in the Cy2 channel, we can stain for acinar cells and ductal cells. Past findings have indicated that fibrosis decreases acinar cells but increases ductal cells. Although EpCAM is an epithelial marker, it is expressed more strongly in ducts more strongly than acini. Interestingly, we observed that over the course of ligation and deligation, the EpCam-FITC stain remained

relatively constant. This could be because the number of acinar cells that are lost are canceled out by the number of ductal cells gained, resulting in a similar area covered by EpCAM. The CD31 stain, stains the endothelial cells within the tissue, which appears to increase at the 14-day ligation timepoint, decrease 3 days following deligation and then increase again. This is also consistent with what we expected because as the tissue becomes more injured and fibrotic, the amount of blood vessels has to increase in order to supply the fibrotic tissue with blood. The amount of blood vessels then decreases when the amount of ECM decreases, and the increase again once the tissue begins to recover. Lastly, the Ki67 stain is at its lowest at the 3-day MOCK condition and with the next lowest condition being the 14-day ligated. This is what we would expect when because the tissue is not injured, i.e., the MOCK condition, and when the tissue has no chance to regenerate, i.e., the 14-day ligated condition, few cells should be proliferating. The Ki67 appears to increase from the 3 day deligated to the 7 day deligated condition suggesting that cells in the salivary gland are beginning to proliferate following deligation. Additionally, we quantified the amount of each stain normalized to the total tissue area. **Figure 8B** is the quantifications for the amount of EpCam-FITC positive area, and once again there is no significant difference across any of the conditions. This is consistent with the image in **Figure 8A** and with past literature. In **Figure 8C**, the amount of CD31 positive area was quantified, and although the levels of CD31 are the highest at the 14-day ligation and 7-day deligation, which is consistent with the images in **Figure 8A**, and past literature, the difference is not significant. In **Figure 8D**, the amount of Ki67 positive area was measured and although there appear to be a huge increase in Ki67 in the 3 day deligated condition, the difference between this condition and the others is not significantly important. The overall trend in Ki67 levels, extremely low at 3-day MOCK and 14-day ligation, with an increase at 3 days post deligation, is promising for future

studies. In **Figure 8E** the amount of DAPI, or cell nuclei, stain was quantified and there was no significant difference between any condition. This is what we expect to see, as the number of cells in the tissue sample should not be changing.

This experiment suggests that the salivary gland is beginning to recover from fibrotic injury starting at 3 days post deligation. As our goal was to determine at what timepoint the ECs are proliferating, we will need to compare the overlap between the Ki76 proliferation marker and CD31, the endothelial cell marker to determine when there are proliferating cells. Although most of our data did not have any significance, our data suggests that 3 days appears to be too early, and by 7 days the ECs appear to be increasing in area, which may be due to proliferation, which we can confirm by counting Ki67+ ECs. As our next step is to perform single cell sequencing on endothelial cells at a timepoint prior to cell proliferation, these data suggest that an intermediate time pint between 3 and 7 days may be ideal for examining angiocrine factors produced by ECs and their contributions to salivary gland regeneration.

Chapter 4: Conclusions and Future Directions

4.1 Conclusions

The study in chapter 3, enables us to examine the ligation/deligation model using mouse salivary glands. Throughout this study, this model has been beneficial in inducing injury in the salivary glands and allows us to study on the molecular level how the salivary glands are transforming when injured.

Chapter 3 suggested the timepoint when the ECs are being to proliferate in the ductal ligation model, 3 days post deligation. This was determined through IHC staining with the markers CD31 and Ki67. Ki67 levels allowed us to pinpoint when proliferation is occurring in the positively stained cells. Through trichrome staining we were able to determine that after 14 days of being ligated the glands had the most ECM, meaning they had the most amount of fibrotic tissue. Once the glands were deligated, the amount of ECM decreased, showing that the amount of injured, fibrotic tissue decreased. Although none of our quantifications were significant, they are promising for more experiments moving forward. All of the data from experiment 1; need larger sample sizes in order to determine significance and accurately determine how ConA and AQP5 vary with injury. The data from experiment 2 suggest that 3 days post deligation is a good time point to begin examining the regeneration of the salivary glands. In future work, we will quantify the co-positivity of Ki67 with the specific cell types with manual counting.

4.2 Future Directions

After completing the experiments in chapter 3, there are still many studies we need to do in order to confirm the time point for when the endothelial cells are proliferating following deligation. We would like to find better methodologies for evaluating successful ligation, more specifically experiment with various saliva collection techniques. We will also need to quantify the amount of CD31 and Ki67 co-positive cells. This will tell us when the endothelial cells specifically are beginning to proliferate following ligation. In addition to examining CD31 co-positivity with Ki67, we will also be examining EpCAM-FITC, AQP5 and DAPI co-positive cells with Ki67. This will enable us to assess the acinar cell proliferative response to deligation. Here, we specifically focused on 3-day data, but moving forward we will examine the 7-day tissue. Previous research conducted by Contorneo discovered that acinar cells were found starting to recover at about 5 days and were further recovered by day 7 via IHC staining for AQP5. To examine how much the acinar cells are recovering at these two time points, we will do more IHC staining and compare the AQP5 levels and glycoprotein levels at both 3 and 7 days. In the future we also plan to trichrome stain 3 and 7 day deligated tissue with specific stains for acinar cell markers. This will allow for us to determine the relationship between acinar cell markers recovery and reduction in fibrosis. We completed IHC and trichrome quantifications in order to pinpoint when the cells are beginning to proliferate, and in the future, we will use single cell RNA sequencing to determine what angiocrine factors produced by endothelial cells are contributing to the regrowth of glands following regeneration. This single cell RNA sequencing will enable us in the future to study these factors and determine potential new therapeutics for individuals suffering from SS.

References

Aure, M., Konieczny, S., & Ovitt, C. (2015). Salivary gland homeostasis is maintained through acinar cell self-Duplication. *Developmental Cell, 33*(2), 231-237. https://doi.org/10.1016/j.devcel.2015.02.013

Cotroneo, E., Proctor, G. B., Paterson, K. L., & Carpenter, G. H. (2008). Early markers of regeneration following ductal ligation in rat submandibular gland. *Cell and Tissue Research, 332*(2), 227-235. https://doi.org/10.1007/s00441-008-0588-6

Ding, B. S., Nolan, D. J., Butler, J. M., James, D., Babazadeh, A. O., Rosenwaks, Z., Mittal, V., Kobayashi, H., Shido, K., Lyden, D., Sato, T. N., Rabbany, S. Y., & Rafii, S. (2010). Inductive angiocrine signals from sinusoidal endothelium are required for liver regeneration. *Nature, 468*(7321), 310–315. https://doi.org/10.1038/nature09493

Holmberg, K. V., & Hoffman, M. P. (2014). Anatomy, biogenesis, and regeneration of salivary glands. *Monographs in Oral Science, 24*, 1–13. https://doi.org/10.1159/000358776

Iorgulescu G. (2009). Saliva between normal and pathological. Important factors in determining systemic and oral health. *Journal of Medicine and Life, 2*(3), 303–307.

Kuriki, Y., Liu, Y., Xia, D., Gjerde, E. M., Khalili, S., Mui, B., Zheng, C., & Tran, S. D. (2011). Cannulation of the mouse submandibular salivary gland via the Wharton's duct. *Journal of Visualized Experiments, 51*, 3074. https://doi.org/10.3791/3074

Kwon, H. R., Nelson, D. A., Desantis, K. A., Morrissey, J. M., & Larsen, M. (2017). Endothelial cell regulation of salivary gland epithelial patterning. *Development, 144*(2), 211-220. https://doi.org10.1242/dev.142497

Luitje, M. E., Israel, A. K., Cummings, M. A., Giampoli, E. J., Allen, P. D., Newlands, S. D., & Ovitt, C. E. (2021). Long-term maintenance of acinar cells in human submandibular

glands after radiation therapy. *International Journal of Radiation Oncology, Biology, Physics*, *109*(4), 1028–1039. https://doi.org/10.1016/j.ijrobp.2020.10.037

Niemela, R. K., Takalo, R., Paakko, E., Suramo, I., Paivansalo, M., Salo, T., & Hakala, M. (July 2004). Ultrasonography of salivary glands in primary Sjögren's syndrome. A comparison with magnetic resonance imaging and magnetic resonance sialography of parotid glands. *Rheumatology*, *43*(7), 875-879. https://doi.org/10.1093/rheumatology/keh187

Nolan, D. J., Ginsberg, M., Israely, E., Palikuqi, B., Poulos, M. G., James, D., Ding, B.-S., Schachterle, W., Liu, Y., Rosenwaks, Z., Butler, Jason M., Xiang, J., Rafii, A., Shido, K., Rabbany, Sina Y., Elemento, O., & Rafii, S. (2013). Molecular signatures of tissue-specific microvascular endothelial cell heterogeneity in organ maintenance and regeneration. *Developmental Cell*, *26*(2), 204–219. https://doi.org/10.1016/j.devcel.2013.06.017

Osailan, S. M., Proctor, G. B., Carpenter, G. H., Paterson, K. L., & Mcgurk, M. (2006). Recovery of rat submandibular salivary gland function following removal of obstruction: A sialometrical and sialochemical study. *International Journal of Experimental Pathology*, *87*(6), 411-423. https://doi.org/10.1111/j.1365-2613.2006. 00500.x

Rafii, S., Butler, J. M., & Ding, B. (2016). Angiocrine functions of organ-specific endothelial cells. *Nature*, *529*(7586), 316-325. https://doi:10.1038/nature17040

Sezis Demirci, M., Karabulut, G., Gungor, O., Celtik, A., Ok, E., & Kabasakal, Y. (2016). Is there an increased arterial stiffness in patients with primary Sjögren's syndrome? *Internal Medicine*, *55*(5), 455–459. https://doi.org/10.2169/internalmedicine.55.3472

Siegel, R. L., Miller, K. D., Fedewa, S. A., Ahnen, D. J., Meester, R. G. S., Barzi, A., & Jemal, A. (2017). Colorectal cancer statistics, 2017. *CA: A Cancer Journal for Clinicians*, *67*(3), 177–193. https://doi.org/10.3322/caac.21395

Shiboski, C. H., Shiboski, S. C., Seror, R., Criswell, L. A., Labetoulle, M., Lietman, T. M., Rasmussen, A., Scofield, H., Vitali, C., Bowman, S. J., & Mariette, X. (2016). 2016 American College of Rheumatology/European League against Rheumatism classification criteria for primary Sjögren's syndrome. *Annals of the Rheumatic Diseases*, *76*(1), 9–16. https://doi.org/10.1136/annrheumdis-2016-210571

Sörensen, I., Adams, R. H., & Gossler, A. (2009). DLL1-mediated Notch activation regulates endothelial identity in mouse fetal arteries. *Blood*, *113*(22), 5680–5688. https://doi.org/10.1182/blood-2008-08-174508

Tan, E. C. K., Lexomboon, D., Sandborgh-Englund, G., Haasum, Y., & Johnell, K. (2017). Medications that Cause dry mouth as an adverse effect in older people: A systematic review and metaanalysis. *Journal of the American Geriatrics Society*, *66*(1), 76–84. https://doi.org/10.1111/jgs.15151

Tektonidou, M., Kaskani, E., Skopouli, F. N., & Moutsopoulos, H. M. (1999). Microvascular abnormalities in Sjögren's syndrome: Nailfold capillaroscopy. *Rheumatology*, *38*(9), 826–830. https://doi.org/10.1093/rheumatology/38.9.826

Tincani, A., Andreoli, L., Cavazzana, I., Doria, A., Favero, M., Fenini, M.-G., Franceschini, F., Lojacono, A., Nascimbeni, G., Santoro, A., Semeraro, F., Toniati, P., & Shoenfeld, Y. (2013). Novel aspects of Sjögren's syndrome in 2012. *BMC Medicine*, *11*(1). https://doi.org/10.1186/1741-7015-11-93

Woods, L. T., Camden, J. M., El-Sayed, F. G., Khalafalla, M. G., Petris, M. J., Erb, L., & Weisman, G. A. (2015). Increased expression of TGF-β signaling components in a mouse model of fibrosis induced by submandibular gland duct ligation. *PloS one*, *10*(5), e0123641. https://doi.org/10.1371/journal.pone.0123641

Wu, A. J. (2015). Management of salivary hypofunction in Sjogren's syndrome. *Current Treatment Options in Rheumatology*, *1*(3), 255–268. https://doi.org/10.1007/s40674-015-0023-6

Xu, J., Wang, D., Liu, D., Fan, Z., Zhang, H., Liu, O., Ding, G., Gao, R., Zhang, C., Ding, Y., Bromberg, J. S., Chen, W., Sun, L., & Wang, S. (2012). Allogeneic mesenchymal stem cell treatment alleviates experimental and clinical Sjögren syndrome. *Blood*, *120*(15), 3142–3151. https://doi.org/10.1182/blood-2011-11-391144

Yeh S. A. (2010). Radiotherapy for head and neck cancer. *Seminars in Plastic Surgery*, *24*(2), 127–136. https://doi.org/10.1055/s-0030-1255330